N91-21210

CRITICAL SPEEDS and FORCED RESPONSE SOLUTIONS for ACTIVE MAGNETIC BEARING TURBOMACHINERY, Part II

D. Rawal, J. Keesee, R. Gordon Kirk
Virginia Polytechnic Institute and State University
Department of Mechanical Engineering
Randolph Hall
Blacksburg
VA 24061-0238

CRITICAL SPEEDS AND FORCED RESPONSE SOLUTIONS FOR ACTIVE MAGNETIC BEARING TURBOMACHINERY PART II

D. Rawal, Research Assistant
J. Keesee, Research Assistant
R. G. Kirk, Associate Professor

Virginia Polytechnic Institute and State University
Blacksburg, VA

ABSTRACT

The need for better performance of turbomachinery with active magnetic bearings has necessitated a study of such systems for accurate prediction of their vibrational characteristics. This is the second part of a two part paper on the effect of sensor location on the forced response characteristics of AMB turbomachinery. This paper presents a modification of existing transfer matrix methods for rotor analysis, to predict the response of rotor systems with active magnetic bearings. The position of the magnetic bearing sensors is taken into account and the effect of changing sensor position on the vibrational characteristics of rotor systems is studied. The modified algorithm is validated using a simpler Jeffcott model described in part I of this paper. The effect of changing from a rotating unbalance excitation to a constant excitation in a single plane is also studied. A typical eight stage centrifugal compressor rotor is analysed using the modified transfer matrix code. The results for a two mass Jeffcott model are presented in part I of this paper. The results obtained by running this model with the transfer matrix method have been compared with the results of the Jeffcott analysis for purposes of verification. Also included, are plots of amplitude vs frequency for the eight stage centrifugal compressor rotor. These plots will demonstrate the significant influence that sensor location has on the amplitude and critical frequencies of the rotor system.

NOMENCLATURE

E	Modulus of elasticity (N/mm^2)
I	Moment of inertia of massless shaft (mm^4)
I_p	Polar moment of inertia (mm^4)
I_t	Transverse moment of inertia (mm^4)
K	Stiffness ratio, k_1/k_2 (dim)
	Stiffness in transfer matrix equations (N/mm)
k_1	AMB stiffness (N/mm)
k_2	Shaft stiffness (N/mm)
M	Mass ratio, m_1/m_2 (dim)
M_{xc}	Moment component in transfer matrix equation (N-mm^2)
M_{xs}	Moment component in transfer matrix equation (N-mm^2)
V_{xc}	Shear component in transfer matrix equation (N)
V_{xs}	Shear component in transfer matrix equation (N)
a_x	Eccentricity component in transfer matrix equation (mm)
a_y	Eccentricity component in transfer matrix equation (mm)
C	Damping (N-sec/mm)
e	Exponential constant = 2.7182818 (dim)
i	Complex constant (dim)
l	Length of massless shafts in transfer matrix equation (mm)
m_i	Point masses in transfer matrix equations (Kg)
xc	Deflection component in transfer matrix equations (mm)
xs	Deflection component in transfer matrix equations (mm)
θ_{xc}	Slope component in the transfer matrix equation (rad)
θ_{xs}	Slope component in the transfer matrix equation (rad)
$F\phi$	Constant excitation force in Jeffcott model (N)
F_{xc}	Constant excitation force component in the transfer matrix equations (N)
F_{xs}	Constant excitation force component in the transfer matrix equations (N)
α	Ratio of the distance between bearing centerline and sensor to half-span of the rotor (dim)
ω	Frequency of shaft excitation (rad/sec)

s	Frequency of shaft rotation (rad/sec)

Subscripts

i	Rotor station number in transfer matrix equations

INTRODUCTION

The use of active magnetic bearings in turbomachinery is a comparatively new development but one which has shown great promise for better control of rotating equipment. The idea behind these bearings is not new however. The use of magnetic attraction to levitate the rotor shaft free of the bearing had been tried before, but because the system is inherently unstable unless a real-time control system is used, the use was not successful. The first actively controlled bearing was developed in the 1950's. Since then the use of active magnetic bearings has gained widespread acceptance particularly in North America and Canada. Weise [2] has given some examples of the varied uses to which active magnetic bearings have been applied. Kirk [5] lists a number of turbomachinery installations where active magnetic bearings have been used. Magnetic bearings possess a number of advantages compared to conventional bearings. They give an almost unlimited control over rotor vibrational characteristics due to adjustable stiffness and damping. Automatic balancing is possible by allowing the rotor to spin on its inertial axis. This leads to decreased vibrations and noise. Active magnetic bearings do not require lubrication, and since they are non-contact bearings, they eliminate the possibility of wear and tear of the stator and rotor surfaces. Weise [2] demonstrates the tolerance of magnetic bearings to a wide range of temperatures and also their insensitivity to hostile environments. Zlotykamien [1] gives a good description of the various advantages of active magnetic bearings.

Most of the research in active magnetic bearings has been in the control systems used. Schweitzer [7] shows a method for controlling an elastic rotor so that it can be represented by a low order model amenable to control techniques. Williams, Keith and Allaire [6] have developed theoretical relationships to relate the characteristics of a controller transfer function to the stiffness and damping properties of an active magnetic bearing. Burrows and Sahinkaya [8] have evaluated various strategies for applying a magnetic bearing to control the synchronous vibration of a flexible rotor. Kirk et al [5] have presented results of shop tests on a high speed eight stage centrifugal compressor supported by active magnetic bearings along with some design recommendations. Keesee [3] has examined the effects of sensor position on the critical frequencies of rotors with active magnetic bearing. This work is an extension of Keesee's work to include sensor position effect on forced response vibration amplitudes, using the modified transfer matrix method.

RESEARCH OBJECTIVE

As stated before in the introduction, the sensors are not located at the place where the attraction forces are applied on the rotor shaft, but at some distance away along the axis of the shaft. Due to this "non-colocation" of the sensors from the bearing position, the deflection sensed by the sensors is not the same as the actual deflection at the bearing but differs from it by some magnitude, dictated by the mode shape of the rotor shaft. Because of this, the stiffness and damping forces of the active magnetic bearing depend not on the deflection at the bearing location, but on the deflection at the sensor location. For such cases, the vibrational characteristics of the rotor system is different from that obtained using conventional analysis programs. The objective of this research is to take into account, the effect of sensor non-colocation on the vibrational characteristics of rotors with active magnetic bearings.

This research is an extension of the work done by Keesee [3] and involves the modification of an existing transfer matrix code to account for sensor non-colocation. But whereas Keesee's research was limited to studying the effect of sensor non-colocation on critical frequencies, this work also considers sensor non-colocation effects on forced response amplitudes. The other objective of this research was to compare the vibrational characteristics of rotor systems, when they are subject to unbalace excitation with circular synchronous shaft rotation, and constant excitation in one plane with no shaft rotation or whirling. The effect of changing mass ratios and stiffness ratios was also studied.

The modification of the transfer matrix program was validated by comparing its results for the two mass model with the results obtained from a simple program written to specifically analyse the two

mass model described in part I of this paper. A typical eight stage centrifugal compressor rotor model was also analysed using the modified transfer matrix method and its results were compared with the results of the Jeffcott model to verify the trend of behaviour of the rotor system with varying sensor locations.

THE MODIFIED TRANSFER MATRIX METHOD

The first analytical study of flexible rotors using the transfer matrix method was presented by Myklestad and Prohl. The rotor is divided into several discrete masses called stations and these masses are joined by massless flexible shafts. The response of the system is computed by using influence coefficients, and formulating a set of equations. The equations are solved and a final sweep is made to obtain the solution. J. W. Lund analysed the equations involved in the transfer matrix method for the case of elliptic non-synchronous response of the rotor system and wrote a program using these equations to study the vibrational characteristics of rotor systems. The program was subsequently simplified to analyse circular synchronous response of rotor systems. This paper describes the modification of precisely this simplified transfer matrix program written by E. J. Gunter Jr. and R. G. Kirk at the University of Virginia, Charlottesville, Virginia. The modification was done to take into account the non-colocation of sensors in active magnetic bearings.

To understand the classical transfer matrix method, consider a typical rotor section element assumed to be composed of a point mass and a massless elastic shaft to its right.

Consider the forces acting on the mass to formulate the equations required for equilibrium. Referring to figure 1

$$V^R_{xic} = V^L_{xic} + (m_i\omega^2 - K_i)x_{ic} - C_i\omega x_{is} + FXC_i + a_{x_i}m_i\omega^2 \quad [1]$$

$$V^R_{xis} = V^L_{xis} + C_i\omega x_{ic} + (m_i\omega^2 - K_i)x_{is} + FXS_i - a_{y_i}m_i\omega^2 \quad [2]$$

$$M^R_{yic} = M^L_{yic} + (I_p - I_T)\omega^2\,\theta^L_{xic} \quad [3]$$

$$M^R_{yis} = M^L_{yis} + (I_p - I_T)\omega^2\,\theta^L_{xis} \quad [4]$$

$$\theta^R_{xic} = \theta^L_{xic} \quad [5]$$

$$\theta^R_{xis} = \theta^L_{xis} \quad [6]$$

$$x^R_{ic} = x^L_{ic} \quad [7]$$

$$x^R_{is} = x^L_{is} \quad [8]$$

The solution in the Y direction can be obtained from the solution in the X direction since it is assumed that the motion of the shaft is circular. Hence equations in the Y direction are not required. Now consider the equations for the massless elastic shaft of station i. From figure 2

$$V^L_{x\,i+1c} = V^R_{xic} \quad [9]$$

$$V^L_{x\,i+1s} = V^R_{xis} \quad [10]$$

$$M^L_{y\,i+1c} = M^R_{yic} + l_i.V^R_{xic} \quad [11]$$

$$M^L_{y\,i+1s} = M^R_{yis} + l_i.V^R_{xis} \quad [12]$$

$$\theta^L_{x\,i+1c} = \theta^R_{xic} + \frac{l_i^2}{2EI}V^R_{xic} + \frac{l_i}{EI}M^R_{yic} \quad [13]$$

$$\theta^L_{x\,i+1s} = \theta^R_{xis} + \frac{l_i^2}{2EI}V^R_{xis} + \frac{l_i}{EI}M^R_{yis} \quad [14]$$

$$x^L_{i+1c} = x^R_{ic} + l_i.0^R_{xic} + \left(\frac{l_i^3}{6EI} - GN_i\right)V^R_{xic} + \frac{l_i^2}{2EI}M^R_{yic} \quad [15]$$

$$x^L_{i+1s} = x^R_{is} + l_i.0^R_{xis} + \left(\frac{l_i^3}{6EI} - GN_i\right)V^R_{xis} + \frac{l_i^2}{2EI}M^R_{yis} \quad [16]$$

These equations can be presented in matrix form and the matrices are called transfer matrices. As can be seen from this matrix, a correction to account for the shear deformation effect has also been included. The terms of this correction factor are explained below

$$GN_i = \frac{l_i}{a_i.G_i.sf_i} \quad [17]$$

a_i = area of section i
G_i = shear modulus of section i

$$sf_i = \frac{[(7. + .6\mu)(1. + dr^2)^2 + (20. + 12.\mu)dr^2]}{[6.(1. + \mu)(11. + dr^2)^2]} \quad [18]$$

μ is poissons ratio $= E_i/2G_i - 1$
dr_i is the diameter ratio = inner diameter/outer diameter

MODIFICATION FOR SENSOR NON-COLOCATION

Due to sensor non-colocation, at the station representing the bearing location, equations [3.1] and [3.2] are modified as follows

$$V^R_{xic} = V^L_{xic} + m_i\omega^2 x_{ic} - K_i x_{ic_{sen}} - C_i\omega x_{is_{sen}} + FXC_i + a_{x_i}m_i\omega^2 \quad [19]$$

$$V^R_{xis} = V^L_{xis} + C_i\omega x_{ic_{sen}} + m_i\omega^2 x_{is} - K_i x_{is_{sen}} + FXS_i - ay_i m_i\omega^2 \quad [20]$$

The bearing stiffness is multiplied by the deflection sensed at the sensor location instead of the actual deflection at the bearing.

ALGORITHM FOR MODIFICATION DUE TO SENSOR NON-COLOCATION

The modification in the point matrix for the bearing station, due to the sensor non-colocation has already been discussed. However a straight forward sweep of the rotor is possible only in certain cases of sensor location. Upon examination, three cases of sensor location relative to the bearing location can be listed.

1. One sensor before the bearing
2. One sensor after the bearing
3. Two sensors, one each on either side of the bearing.

Case 1
For case 1, the sensor deflections are saved in the sweeping process and then used at the bearing station. The sweeping process is straightforward. Refer figures 3.

Case 2
In this case, since the sensor comes after the bearing, the sensor deflections are not known when the sweeping process reaches the bearing. Thus the sensor deflections are assumed to be some arbitrary value. Generally, the deflections at the station before the bearing are used as these arbitrary values. The sweeping process is then continued until the sensor location is reached. Here a comparison is made between the assumed sensor deflection and the sensor deflection calculated by the sweeping process. If the two quantities agree to within a certain margin of error, the sweeping process is continued from the sensor station onwards. If the two quantities do not lie within the error margin, the program iterates back to the bearing location and uses the sensor deflections calculated by the current sweeping process. These sensor deflections are used, as explained before, in

the bearing station point matrix calculations and the sweep process is continued. This leads to a series of iterations between the bearing station and the sensor station and these iterations are continued until the sensor deflections used at the bearing station agree with the sensor deflections calculated at the sensor station by the sweeping process, *i.e.* convergence is obtained. refer figures 3.

Case 3

With two sensors, one each before and after the bearing, the case can be split up into two cases one resembling case one and the other resembling case two. Refer figures 3. When the sensor before the bearing is reached, the sensor deflections are saved. These are used, the first time the bearing location is reached. The sweep process is then continued and the sensor after the bearing is dealt with in a manner similar to case two.

DISCUSSION OF THE CONVERGENCE PROCESS

To aid the process of convergence to the correct values of sensor deflections, the Taylors series convergence technique in two variables was used. This method was the most suitable one since there is cross-coupling between the stiffness and damping terms. However, due to the very low magnitude derivatives involved, the convergence process fails and leads to divergence from the correct solution.

When the cross-coupling of the stiffness and damping terms was ignored, and the Secant method of convergence was used to converge on the sensor deflections along the two axes independently, the algorithm converged with diminishing oscillations. However the number of iterations required were more than those required, when no convergence algorithm was used.

Thus simply using the sensor deflections obtained from the sweeping process, back at the bearing location, gave the fastest convergence. Refer table 1.

MODIFICATION TO SEPARATE GYROSCOPIC STIFFNESS FROM TRANSVERSE STIFFNESS

When the rotor is subjected to an external vibrational force assuming no unbalance to be present, the gyroscopic stiffness will depend only on the rotor spinning speed and not on the frequency of excitation. Considering the rotor spinning frequency to be "s", equations [3.3] and [3.4] are modified as follows

$$M^R_{yic} = M^L_{yic} + \omega(sI_p - \omega I_T)\theta_{xic} \qquad [21]$$

$$M^R_{yis} = M^L_{yis} + \omega(sI_p - \omega I_T)\theta_{xis} \qquad [22]$$

Here ω is the frequency of excitation.

COMPARISON OF THE RESULTS OF THE 2 MASS ROTOR SYSTEM, FOR THE JEFFCOTT MODEL AND THE TRANSFER MATRIX METHOD

The results of the 2 mass rotor system as obtained by the Jeffcott Model program have already been shown and discussed in part I of this paper. The same rotor system data was used with the modified transfer matrix method program, so as to compare the results with the Jeffcott model and thus validate the correctness of the modifications. The Jeffcott model is important, but because of its simplicity, its results are of limited use. Also it does not model a complex rotor system composed of many disk masses and possibly different shaft cross-sections along the rotor length. Hence, it is the transfer matrix method that is more useful for application purposes, and the Jeffcott model will serve for the purpose of comparison only.

Tables 2 and 3 give the comparison between the two programs. As can be seen from the tables, there is a fairly close agreement between the results obtained from the two programs. The agreement in the critical frequency values is much better than that between amplitude values and again, amplitude values agree better than phase angle values. This is because, the critical frequencies of a rotor system depends mostly on its mass and stiffness properties, both of which are accounted for in a similar manner in the two programs. The amplitude and phase angle values show greater disagreement due to the fact that the Jeffcott code assumes a sine-wave shape for the mode shapes and this assumption is only an approximation of the actual mode shape. It can be seen from the tables, that the Jeffcott code underestimates amplitude values in most cases. Also, amplitude values show a

higher disagreement when a constant force excitation is applied instead of an unbalance force excitation.

THE EIGHT STAGE CENTRIFUGAL COMPRESSOR ROTOR SYSTEM MODEL

To obtain a more realistic idea of the influence of sensor position, an eight stage centrifugal compressor rotor system was used with the transfer matrix code. This rotor system is illustrated in figure 4 and its design parameters are given in table 4.
The program was run with all the four cases of sensor positions, namely sensor colocation, inboard sensors, outboard sensors and two sensors on each side of the bearing. α values of -0.18, 0 and 0.18 were used, as is indicated by the sensor locations.

RESULTS OBTAINED FROM THE EIGHT STAGE COMPRESSOR ROTOR SYSTEM

The results obtained from the eight stage compressor rotor system are summarized below and illustrated in figures 5 to 11.

1. The first mode critical frequency increases as the sensor is moved from the direction of the outboard location in the direction of the inboard location. This is in agreement with the results obtained from the two mass rotor system.

2. A significant difference between these plots and those of the two mass model, is the higher amplitudes exhibited by the compressor rotor system when the sensors are moved inboard. To verify this deviation, an approximate two mass model of the compressor rotor system was run with the Jeffcott program. The results obtained with this approximate model are shown in figures 7 and 8, and show agreement with the results obtained by the transfer matrix program with the compressor rotor system data as input. The reason for this behaviour will become clear when the mode shape shown in figures 9 is examined.
   The deflection at the sensor location is less compared to the deflection at the bearing location. Due to this, a lesser stiffness and damping force is applied at the bearing location and this leads to higher amplitudes of the rotor system. For a certain inboard sensor location, the deflection at the sensor location is reduced to zero and this condition will produce the largest amplitudes in the rotor system. The peculiar first mode shape that produces this phenomenon is similar to that observed in the third mode, and seems to be the result of the high bearing damping values. It has been observed that as sensors are moved inboard, the first critical frequency increases and the third critical frequency decreases. This is shown in figure 10. High bearing damping may bring the first and third critical frequencies together in such a case and thus produce a first mode shape similar to the third mode shape.

3. Additionally, it was observed that when the mass ratio was increased, the maximum amplitudes occured with inboard sensor locations nearer to the bearing location. Refer figures 11. This can also be explained from the plots of the mode shapes. The maximum amplitude is observed when the deflection at the sensor location is zero. In such a case, the stiffness and damping forces at the bearing location are reduced to zero and the rotor system essentially exhibits free-free vibration. Due to this, the deflection along the rotor longitudinal axis will depend only on the mass distribution of the rotor system and not on the bearing stiffness and damping. A higher mass ratio means greater mass at the bearing location and therefore, lesser deflection in free-free vibration than that at midspan. In such a case, the point of zero deflection occurs nearer to the bearing location and a sensor placed at this point will produce the maximum amplitude of vibration of the rotor system.

CONCLUSIONS

The modification of the rotor dynamics codes to account for sensor non-colocation show a definite change in the vibrational characteristics when the sensors are moved away from the bearing location. The following conclusions can be drawn from this research:

1. The first mode critical frequency increases as the sensor is moved from the outboard to the inboard direction. This is due to the fact that for the first mode, the sensors sense a greater deflection as they move inboard and away from the bearing location. This increases the effective stiffness of the active magnetic bearing and results in higher critical frequencies. Because of this effect, it is possible to bypass the first critical by using the inboard sensors while starting the rotor and when the rotational frequency nears the first critical, switching to the outboard

sensors. This has been suggested by Keesee [3]. The higher critical frequencies can be handled similarly.

2. The amplitudes at the first critical will be higher with outboard sensors and decrease as the sensors are moved inboard and away from the bearing. However, this is not true in certain cases where the first and third mode coincide. In such a case, the amplitudes at the first critical increase as the sensors are moved inboard upto a certain point and then decrease again. The reason for such behaviour can be traced to the presense of high damping values along with the condition of inboard sensors. The behaviour of the critical frequencies and amplitudes, with regard to changes in the sensor position, can be predicted by examining the mode shape of the rotor shaft at or near the critical frequencies.

3. The results indicate a fairly close agreement between the Jeffcott model and the transfer matrix model. The comparison indicates greater differences in amplitude values compared to critical frequency values and greater deviation in phase angle values compared to amplitude values.

4. The behaviour of the rotor system, with respect to changes in sensor location, does not indicate any significant deviation when a constant force excitation is used instead of an unbalance force excitation.

5. The effect of sensor location on first mode critical frequency increases with higher stiffness ratios. This has been explained in the second chapter. Higher mass ratios lead to increased damping effects in the third mode and hence lower the amplitudes considerably.

The following recommendations can be made for future work in this area:

1. The transfer matrix model modified for this work, does not consider the effect of pedestal stiffness and damping, *ie* it assumes a rigid foundation. The program can easily be modified to take this factor into account.

2. The existing transfer matrix code can only handle circular synchronous rotation of the rotor system. It can be extended to analyse non-circular and non-synchronous motion of the shaft.

3. The constant force excitation in the transfer matrix program is applied as a force function, directly on the journal mass. The behaviour of the rotor system, when the constant force excitation is applied as a displacement function, and on the bearing or pedestal mass, needs to be investigated.

4. The modified transfer matrix code assumes that no couplings are present in the rotor longitudinal cross-section. The code can be modified for the presence of a coupling, which then, would only transfer displacements and shears across the connection, but would not transfer the moments.

BIBLIOGRAPHY

1. Zlotykamien H., "The Active Magnetic Bearing enables Optimum Control of Machine Vibrations," *International Conference on Vibrations in Rotating Machinery, Proc. of the Institution of Mechanical Engineers,* Sept. 1988

2. Weise D. A., "Present Industrial Applications of Active Magnetic Bearings," *22nd Intersociety Energy Conversion Engineering Conference, American Institute of Aeronautics and Astronautics,* Aug. 1987.

3. Keesee J. M., "Influence of Active Magnetic Bearing Sensor Location on the Calculated Critical Speeds of Turbomachinery," *Masters Thesis, Virginia Polytechnic Institute and State University,* June 1989.

4. Hustak J., Kirk R.G., and Schoeneck K. A., "Active Magnetic Bearings for Optimum Turbomachinery Design," *Instability in Rotating Machinery, NASA Conference Publication 2409,* June 1985

5. Kirk R. G., and Hustak J. F., "Analysis and Test Results of two Centrifugal Compressors using Active Magnetic Bearings," *International Conference on Vibrations in Rotating Machinery, Proc. of the Institution of Mechanical Engineers,* Sept. 1988

6. Williams R. D., Keith F. J., and Allaire P.E., "Digital control of Active Magnetic Bearings," *IEEE Transactions on Industrial Electronics,* Vol. 37, No. 1, Feb. 1990.

7. Schweitzer G., "Magnetic Bearings for Vibration Control," *Instability in Rotating Machinery, NASA Conference Publication 2409,* June 1985.

8. Burrows C. R., and Sahinkaya M. N., "Control Strategies for use with Magnetic Bearings," *International Conference on Vibrations in Rotating Machinery, Proc. of the Institution of Mechanical Engineers,* Sept. 1988.

9. Kirk R.G., and Gunter E. J., "The Effect of Support Flexibility and Damping on the Sunchronous Response of a Single-Mass Flexible Rotor," *ASME Transactions, Journal of Engineering for Industry,* Vol. 94, Series B, No. 1, 1972.

10. Lund J. W., "Stability and Damped Critical Speeds of a Flexible Rotor in Fluid-Film Bearings," *ASME Transactions, Paper No. 73-Det-103, 1973.*

ACKNOWLEDGMENT

This work has been sponsored by a joint industry/Virginia Center for Innovative Technology Research Grant No. CAE-89-015, with matching funds from Dresser-Rand Co. and Magnetic Bearings, Inc. The authors are especially grateful for the support given by Dr. Ira Jacobson, Director of the Institute of Computer Aided Engineering, Charlottesville, Virginia.

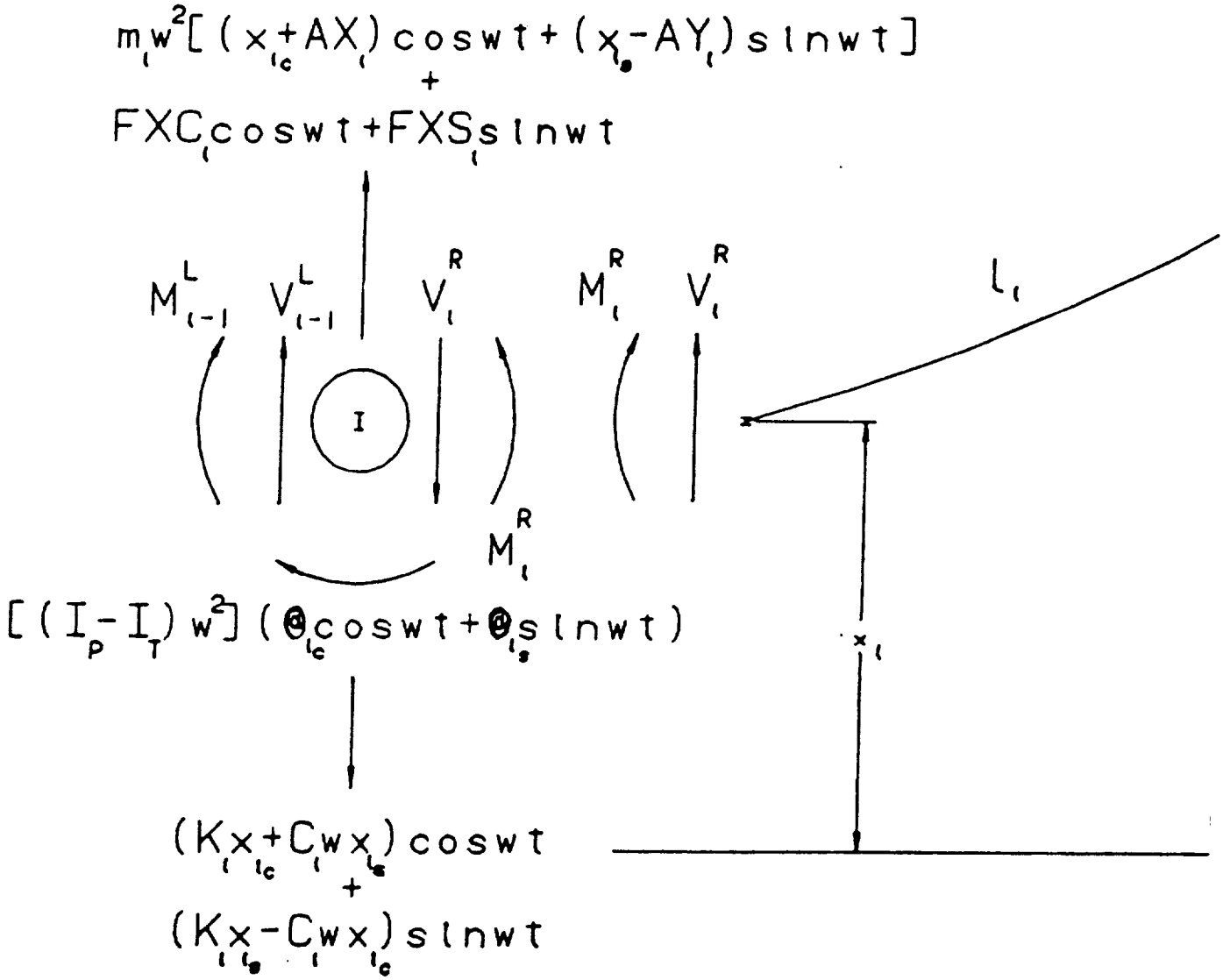

Figure 1. Forces acting on the point mass

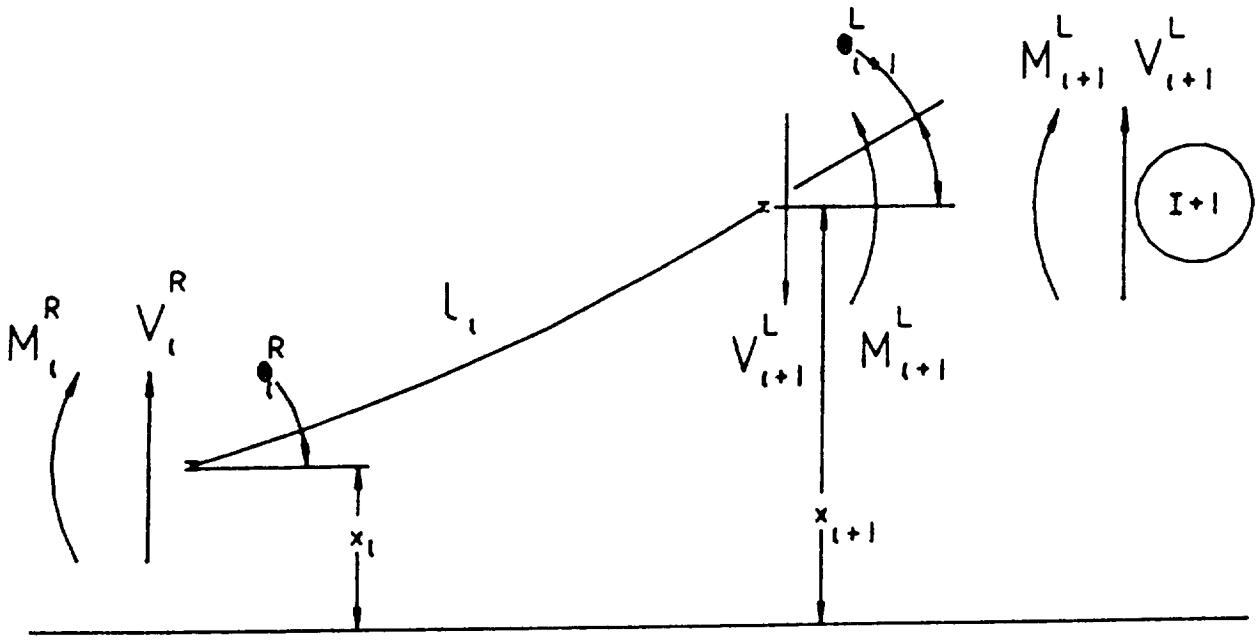

Figure 2. Forces acting on the massless elastic shaft

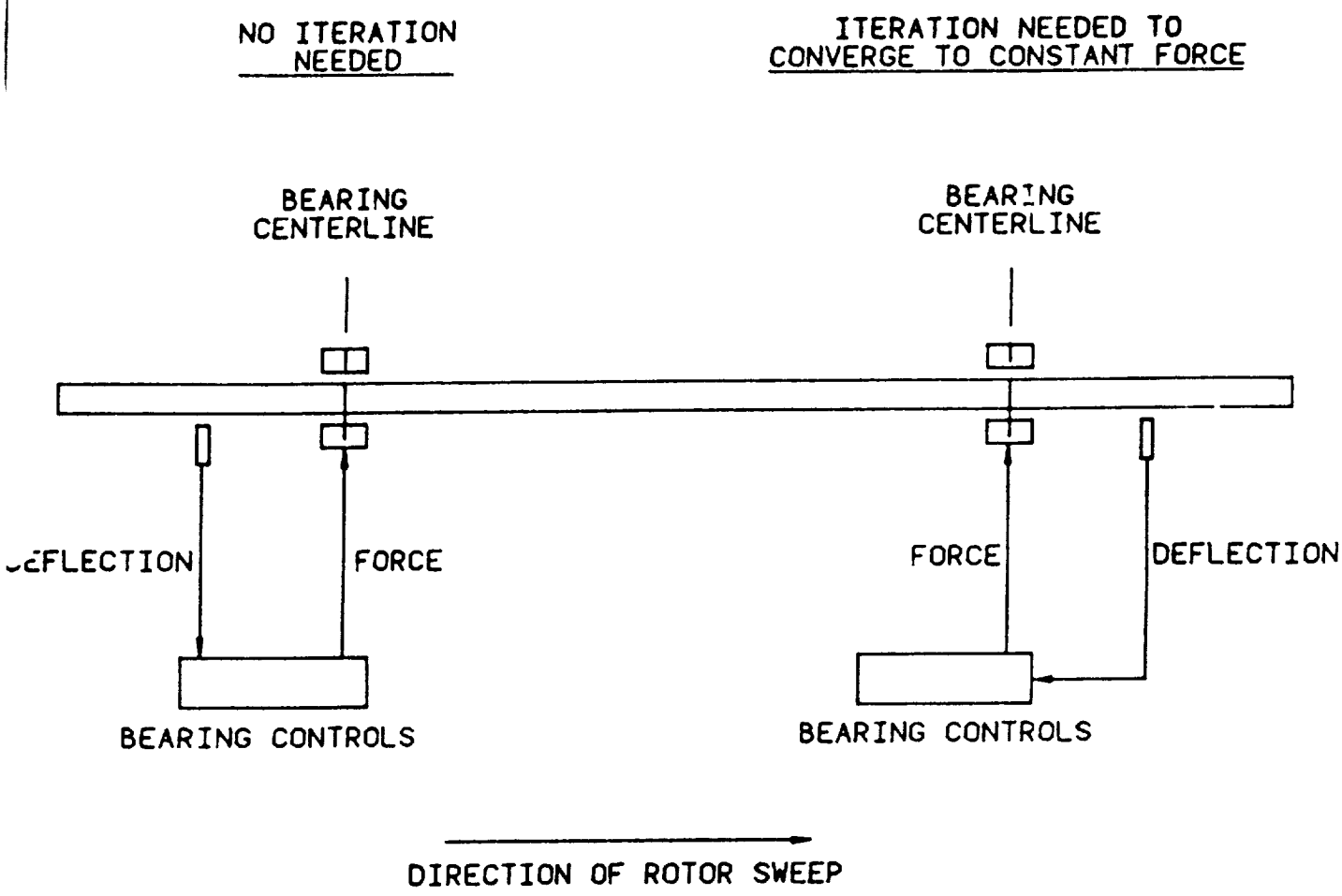

Figure 3. Different sensor locations

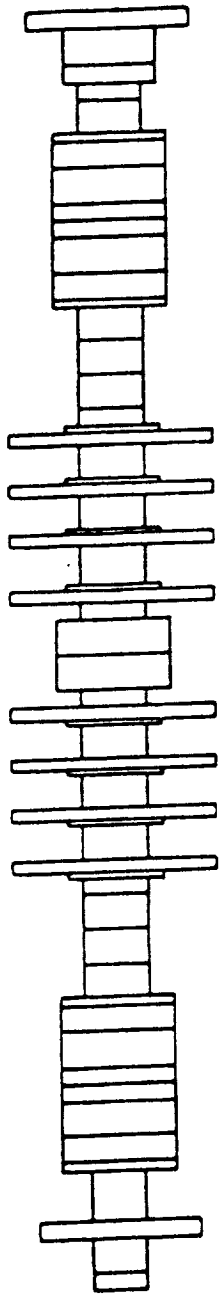

Figure 4. The eight stage centrifugal compressor rotor system

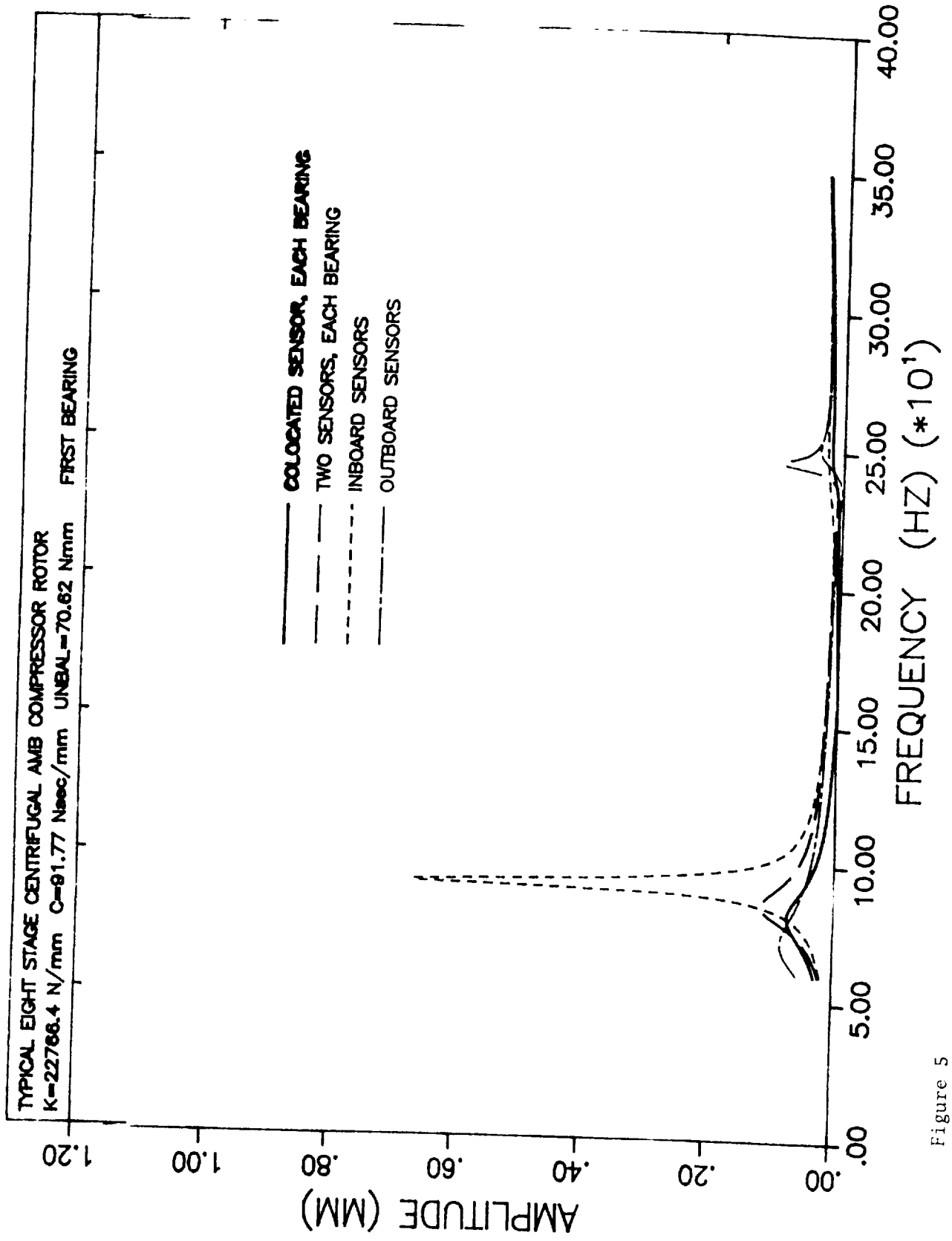
TYPICAL EIGHT STAGE CENTRIFUGAL AMB COMPRESSOR ROTOR
K=22788.4 N/mm C=91.77 Nsec/mm UNBAL=70.62 Nmm FIRST BEARING
COLOCATED SENSOR, EACH BEARING
TWO SENSORS, EACH BEARING
INBOARD SENSORS
OUTBOARD SENSORS
AMPLITUDE (MM)
.00
.20
.40
.60
.80
1.00
1.20
FREQUENCY (HZ) (*10¹)
5.00
10.00
15.00
20.00
25.00
30.00
35.00
40.00

Figure 5

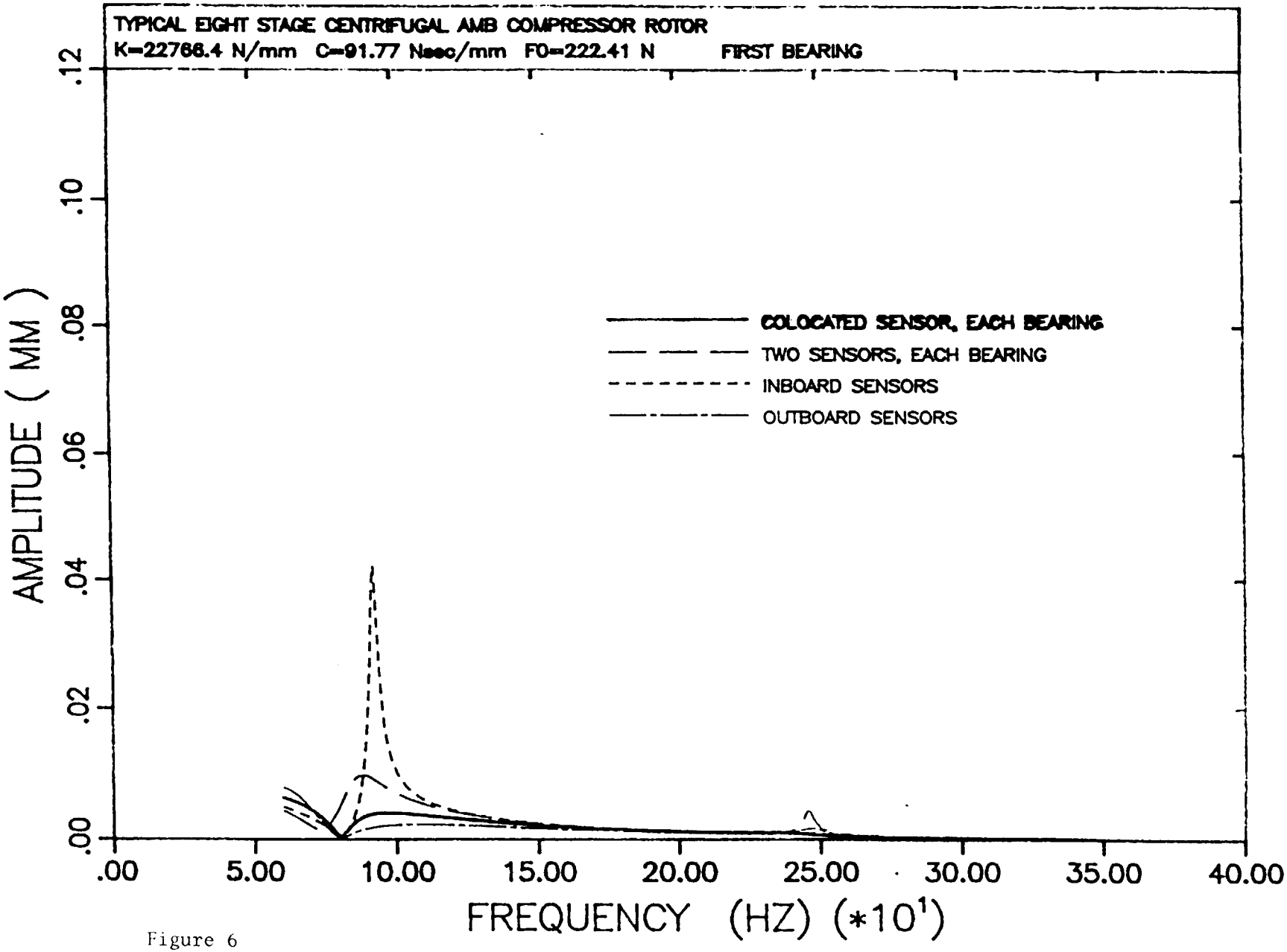
TYPICAL EIGHT STAGE CENTRIFUGAL AMB COMPRESSOR ROTOR
K=22766.4 N/mm C=91.77 Nsec/mm F0=222.41 N FIRST BEARING
COLOCATED SENSOR, EACH BEARING
TWO SENSORS, EACH BEARING
INBOARD SENSORS
OUTBOARD SENSORS
AMPLITUDE (MM)
.00
.02
.04
.06
.08
.10
.12
.00
5.00
10.00
15.00
20.00
25.00
30.00
35.00
40.00
FREQUENCY (HZ) (*10¹)

Figure 6

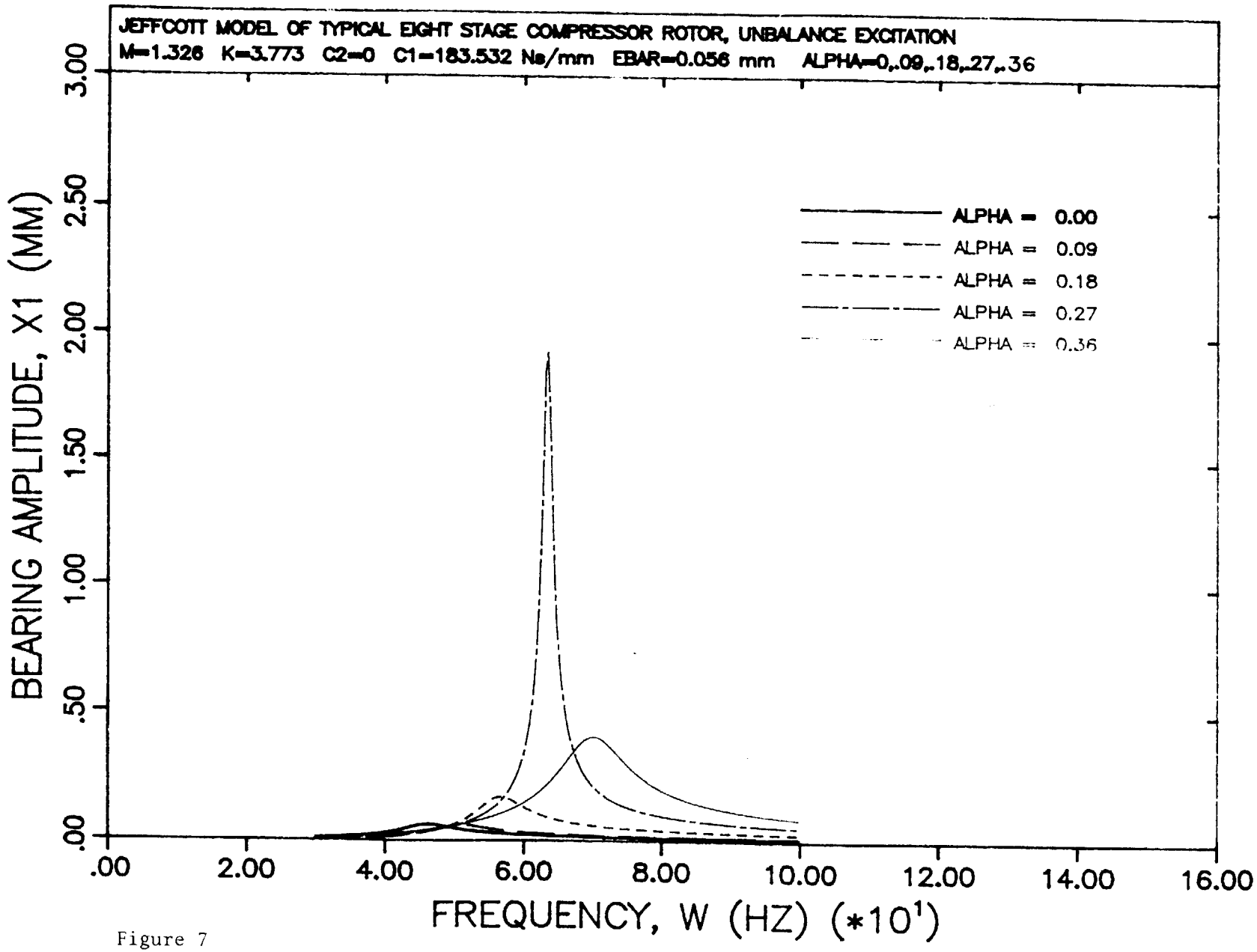
JEFFCOTT MODEL OF TYPICAL EIGHT STAGE COMPRESSOR ROTOR, UNBALANCE EXCITATION
M=1.326 K=3.773 C2=0 C1=183.532 Ns/mm EBAR=0.056 mm ALPHA=0,.09,.18,.27,.36
ALPHA = 0.00
ALPHA = 0.09
ALPHA = 0.18
ALPHA = 0.27
ALPHA = 0.36
BEARING AMPLITUDE, X1 (MM)
.00
.50
1.00
1.50
2.00
2.50
3.00
.00
2.00
4.00
6.00
8.00
10.00
12.00
14.00
16.00
FREQUENCY, W (HZ) (*10¹)

Figure 7

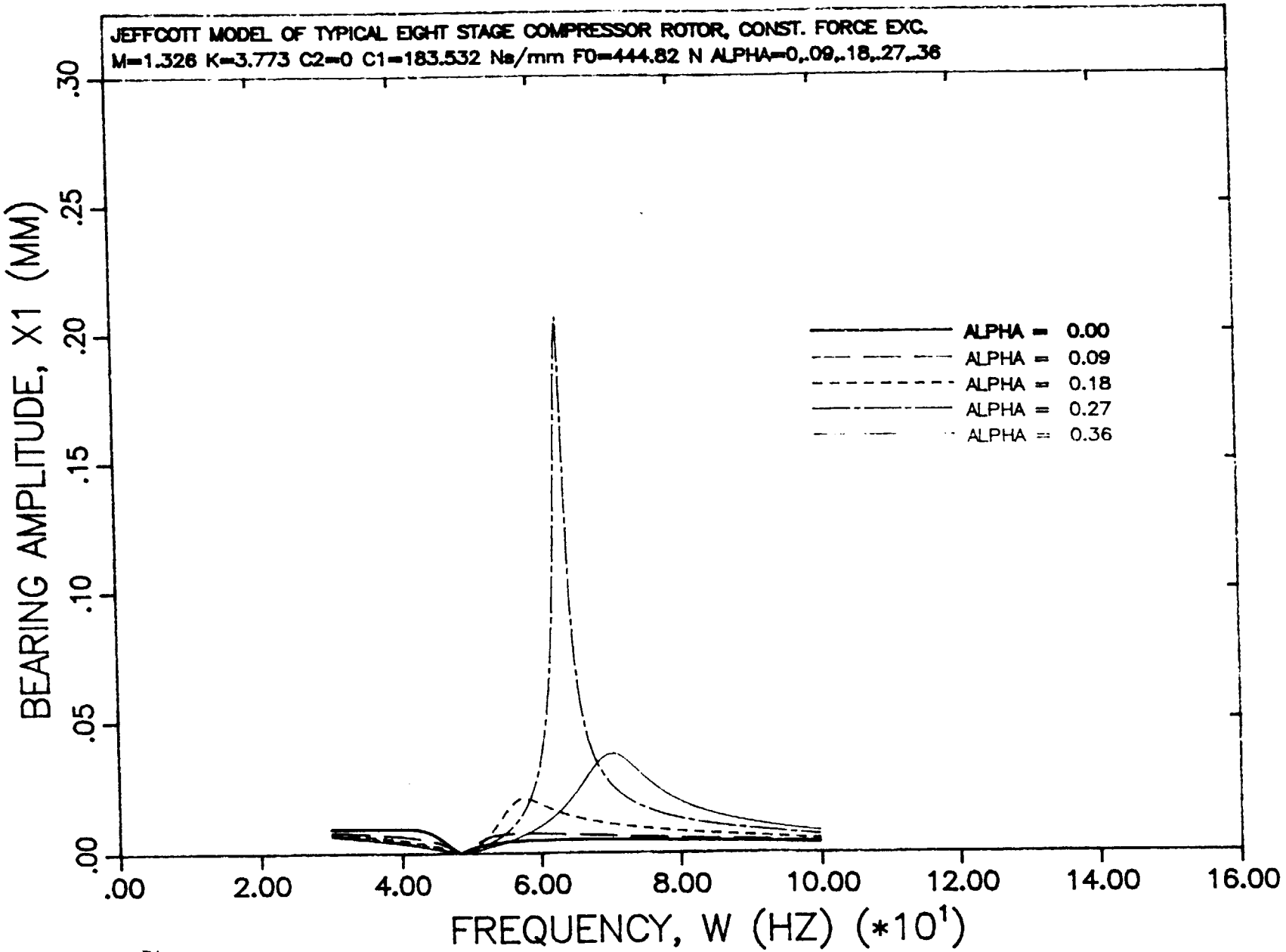
JEFFCOTT MODEL OF TYPICAL EIGHT STAGE COMPRESSOR ROTOR, CONST. FORCE EXC.
M=1.326 K=3.773 C2=0 C1=183.532 Ns/mm F0=444.82 N ALPHA=0,.09,.18,.27,.36
BEARING AMPLITUDE, X1 (MM)
.00
.05
.10
.15
.20
.25
.30
.00
2.00
4.00
6.00
8.00
10.00
12.00
14.00
16.00
FREQUENCY, W (HZ) (*10¹)
ALPHA = 0.00
ALPHA = 0.09
ALPHA = 0.18
ALPHA = 0.27
ALPHA = 0.36

Figure 8

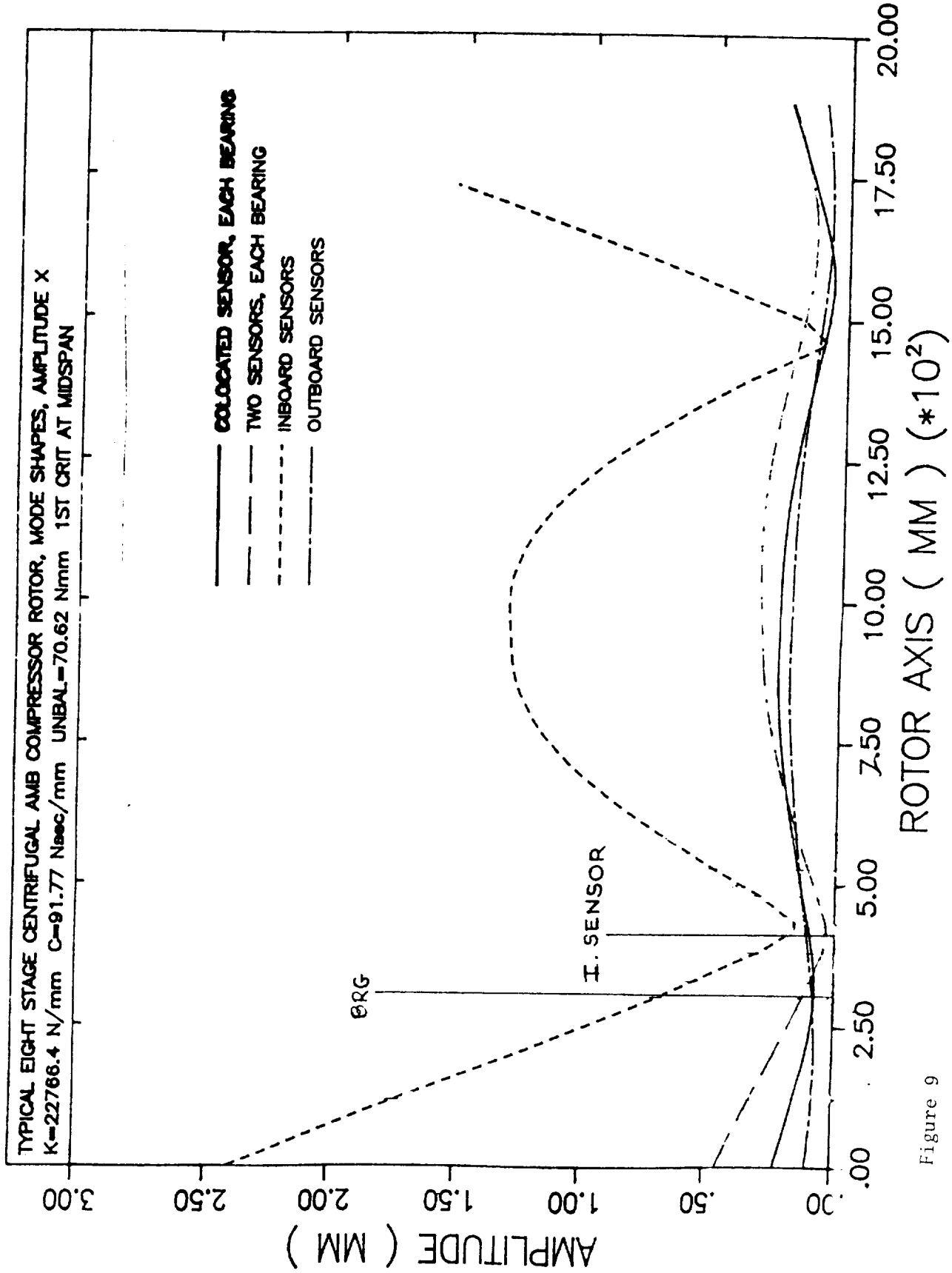
TYPICAL EIGHT STAGE CENTRIFUGAL AMB COMPRESSOR ROTOR, MODE SHAPES, AMPLITUDE X
K=22766.4 N/mm C=91.77 Nsec/mm UNBAL=70.62 Nmm 1ST CRIT AT MIDSPAN
COLOCATED SENSOR, EACH BEARING
TWO SENSORS, EACH BEARING
INBOARD SENSORS
OUTBOARD SENSORS
ØRG
I. SENSOR
AMPLITUDE (MM)
ROTOR AXIS (MM) (*10²)
.00
2.50
5.00
7.50
10.00
12.50
15.00
17.50
20.00
.00
.50
1.00
1.50
2.00
2.50
3.00

Figure 9

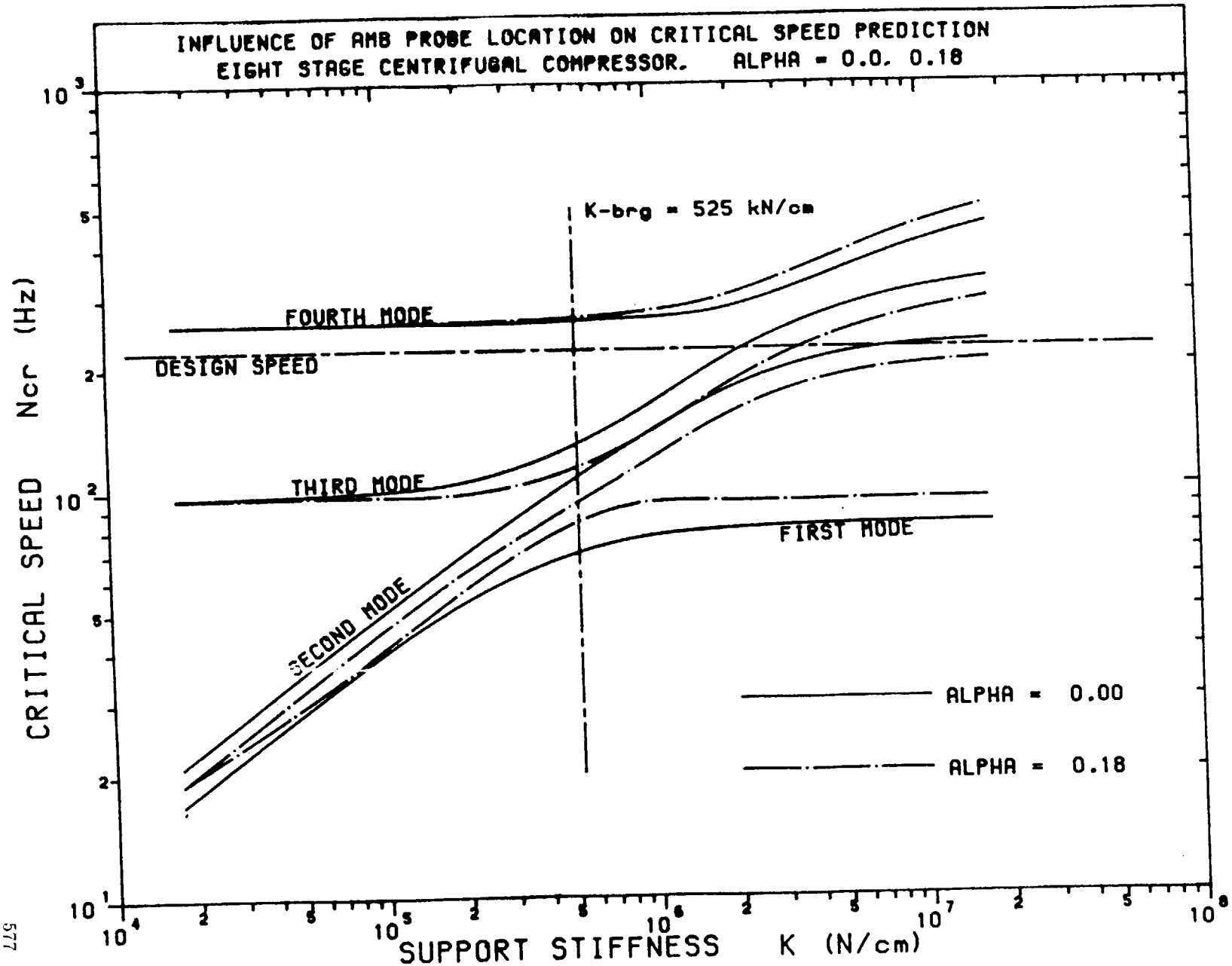
INFLUENCE OF AMB PROBE LOCATION ON CRITICAL SPEED PREDICTION
EIGHT STAGE CENTRIFUGAL COMPRESSOR. ALPHA = 0.0, 0.18
K-brg = 525 kN/cm
FOURTH MODE
DESIGN SPEED
THIRD MODE
FIRST MODE
SECOND MODE
ALPHA = 0.00
ALPHA = 0.18
CRITICAL SPEED Ncr (Hz)
SUPPORT STIFFNESS K (N/cm)

Figure 10

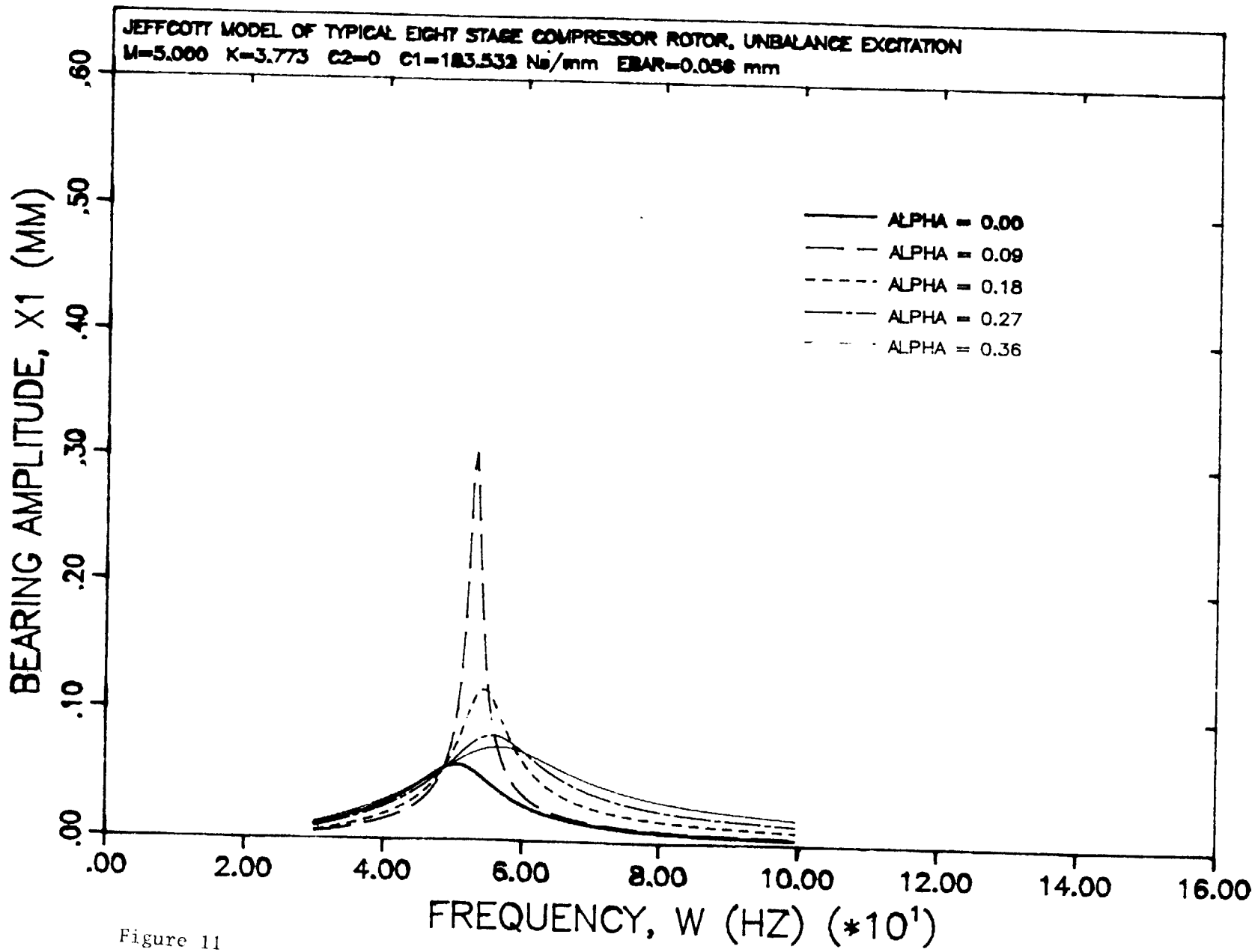
JEFFCOTT MODEL OF TYPICAL EIGHT STAGE COMPRESSOR ROTOR, UNBALANCE EXCITATION
M=5.000 K=3.773 C2=0 C1=183.532 Ns/mm EBAR=0.056 mm
ALPHA = 0.00
ALPHA = 0.09
ALPHA = 0.18
ALPHA = 0.27
ALPHA = 0.36
BEARING AMPLITUDE, X1 (MM)
.00
.10
.20
.30
.40
.50
.60
.00
2.00
4.00
6.00
8.00
10.00
12.00
14.00
16.00
FREQUENCY, W (HZ) (*10¹)

Figure 11

2 MASS MODEL, UNBALANCE EXCITATION, M = 1, K = 2, ALPHA = 0.3 FREQ = 130 HZ, CONVERGENCE TO XC, TRUE SOLUTION = 7.649442						
No. of Iter.	Taylor's series Convergence	% Diff. from true Soln.	Secant method Convergence	% Diff. from true Soln.	Simple Iteration	% Diff. from true Soln.
1	3.500004	54.24	3.500004	54.24	3.500004	54.24
2	8.051951	-5.26	8.051951	-5.26	8.051951	-5.26
3	7.737319	-1.15	7.737319	-1.15	7.737319	-1.15
4	7.581234	0.89	7.930811	-3.68	7.628863	0.27
5	7.849375	-2.61	7.605373	0.576	7.648726	0.0094
6	3.625942	52.60	7.642738	0.088	7.650135	-0.0091
7	69.54724	-809.2	7.655252	-0.076	7.649398	0.00058
8	-959.629	12645.1	7.650030	-0.0077	7.649425	0.00022
9	15109.55	-197425	7.649057	0.0050	7.649445	-0.00004
10	-235777.3	3082381	7.649363	0.001	7.649442	0.0
11	3681287.0	-48124809	7.649458	-0.00021	7.649442	0.0
12	---	---	7.649447	-0.000065	7.649442	0.0
13	---	---	7.649434	0.0001	7.649442	0.0
14	---	---	7.649441	0.000013	7.649442	0.0
15	---	---	7.649443	-0.000013	7.649442	0.0
16	---	---	7.649442	0.0	7.649442	0.0
17	---	---	7.649441	0.000013	7.649442	0.0
18	---	---	7.649441	0.000013	7.649442	0.0
19	---	---	7.649442	0.0	7.649442	0.0

Table 1. Comparison of different convergence schemes

FIRST MODE, UNBALANCE EXCITATION, M = 1, K = 2, BEARING/(MIDSPAN)			
	Jeffcott Code	Transfer matrix Code	% Difference
α = -0.2 Critical Frequency Amplitude Phase Angle	32.167 / (32.167) 2.285 / (4.425) 103.48 / (102.57)	32.167 / (32.167) 2.302 / (4.482) 86 / (85.1)	0 / (0) -0.74 / (-1.29) 16.89 / (17.03)
α = 0.0 Critical Frequency Amplitude Phase Angle	35.333 / (35.333) 1.408 / (3.401) 90.214 / (88.398)	35.333 / (35.333) 1.408 / (3.402) 91.6 / (89.8)	0 / (0) 0 / (-0.03) -1.54 / (-1.59)
α = 0.2 Critical Frequency Amplitude Phase Angle	40.333 / (40.333) 0.539 / (2.281) 92.571 / (86.391)	40.167 / (40.000) 0.571 / (2.310) 104.1 / (81.8)	0.41 / (0.83) -5.94 / (-1.27) -12.45 / (5.31)

Table 2. Comparison of the results of the 2 mass rotor system, for the Jeffcott model and the transfer matrix method

FIRST MODE, CONSTANT FORCE EXCITATION, M = 1, K = 2, BEARING/(MIDSPAN)			
	Jeffcott Code	Transfer matrix Code	% Difference
α = -0.2 Critical Frequency Amplitude Phase Angle	32.167 / (32.167) 4.577 / (8.896) 104.24 / (104.24)	32.167 / (32.167) 5.410 / (10.522) 86.8 / (86.8)	0 / (0) -18.20 / (-18.28) 16.73 / (16.73)
α = 0.0 Critical Frequency Amplitude Phase Angle	35.333 / (35.333) 3.045 / (7.352) 90.214 / (90.214)	35.333 / (35.333) 3.262 / (7.882) 91.6 / (91.6)	0 / (0) -7.13 / (-7.21) -1.54 / (-1.54)
α = 0.2 Critical Frequency Amplitude Phase Angle	40.333 / (40.333) 1.335 / (5.643) 88.527 / (88.527)	40.000 / (40.000) 1.420 / (5.709) 83.9 / (83.9)	0.83 / (0.83) -6.37 / (-1.17) 5.23 / (5.23)

Table 3. Comparison of the results of the 2 mass rotor system, for the Jeffcott model and the transfer matrix method

ROTOR SYSTEM PROPERTY	SI UNITS	ENGLISH UNITS
Total rotor length	*1879.6 mm*	*74.0 in*
Distance to bearing 1 centerline	*304.8 mm*	*12.0 in*
Distance to sensor at bearing 1:		
Outboard sensor	*190.5 mm*	*7.5 in*
Inboard sensor	*419.1 mm*	*16.5 in*
Distance to bearing 2 centerline	*1574.8 mm*	*62.0 in*
Distance to sensor at bearing 2:		
Inboard sensor	*1460.5 mm*	*57.5 in*
Outboard sensor	*1689.1 mm*	*66.5 in*
Mid-span diameter	*177.8 mm*	*7.0 in*
Journal diameter	*177.8 mm*	*7.0 in*
Journal length	*254.0 mm*	*10.0 in*
Total rotor weight	*2.95 KN*	*663.2* lb_f
Reaction at bearing 1	*1.41 KN*	*317.0* lb_f
Reaction at bearing 2	*1.54 KN*	*346.2* lb_f

Table 4. Data for eight stage centrifugal rotor system model